

CHAPTER IV

ELECTROSPUN DOXY-H LOADED-POLY(ACRYLIC ACID) NANOFIBER MATS: IN VITRO DRUG RELEASE AND ANTIBACTERIAL PROPERTIES INVESTIGATION

4.1 Abstract

Electrospun DOXY-h loaded-poly(acrylic acid) nanofiber mats (PAA/DOXY-h nanofiber mats) were prepared by the electrospinning technique and post-spinning sorption method at various doses: PAA/DOXY-h125, PAA/DOXY-h250, PAA/DOXY-h500, and PAA/DOXY-h1000. The morphology, drug content, release characteristics, and antibacterial activities of the PAA/DOXY-h nanofiber mats were investigated with scanning electron microscopy, UV-Visible spectrophotometry and disc diffusion methodology. The PAA/DOXY-h nanofiber mats had a diameter range of 285-340 nm, and a smooth surface without beads. Adsorption isotherms of DOXY-h could be described well with the Freundlich model. The amounts of DOXY-h, after the post-spinning sorption process, in the PAA/DOXY-h nanofiber mats ranged between 27.57 mg/g to 101.71 mg/g. All of the PAA/DOXY-h nanofiber mats exhibited an initial burst release characteristic with cumulative releasing percentages between 37.14% and 45.97%, which followed the Fickian diffusion mechanism. Based on the antibacterial investigation, the tested gram-positive bacteria, *Staphylococcus aureus* and *Streptococcus agalactiae*, seemed to be more sensitive to PAA/DOXY-h nanofiber mats than the tested gram-negative bacteria, *Pseudomonas aeruginosa*. These PAA/DOXY-h nanofiber mats could be used as an antibacterial wound dressing.

Keywords: poly(acrylic acid) nanofiber mats; doxycycline hyclate; electrospinning; in vitro drug release

4.2 Introduction

Microbes on the human skin are divided into three general categories: pathogens, potential pathogens, and harmless symbiotic organisms [1]. Bacteria are

one of these cutaneous microbes. Normal bacteria that are commonly found on the skin include *Staphylococcus epidermidis*, corynebacterium, propionibacterium, occasionally *Staphylococcus aureus*, and peptostreptococcus species [2]. Some of the aforementioned cutaneous bacteria, which are known as opportunistic pathogens, can become pathogenic when the human immune system is weakened, or when there are concurrent infections and illnesses such as cancer [3]. They can infect the human body and cause many diseases.

When the human skin barrier is removed or damaged, chances of more serious infections and issues increase. The application of a wound dressing has been practiced in order to protect the wound from contaminants as well as absorb exudate, reduce infections, and promote wound healing [4]. Among the many types of wound dressing materials, a nanofibrous wound dressing may offer superior benefits over conventional dressing materials. Nanofiber mats have drawn more research attention due to their advantages. These advantages include extremely high specific surface area, non-woven form with microporous structure that is effective against bacterial permeation and attraction of fibroblasts to the dermis, which are necessary for the repair of damaged tissues [5]. In addition, these mats can be cut into any size or shape, are non-irritating, attractive in appearance, practical and comfortable, all of which makes this type of dressing an appealing alternative. These advanced properties of nanofibers, thereby, make them to be a good candidate for tissue engineering, sensors, filters, wound dressing materials, and drug delivery systems [6-10].

Electrospinning is a technique widely used to fabricate nanofibers. Outstanding characteristics such as a simple and easy production process, relatively low price, and high flexibility make nanofiber mats, produced from this technique, more attractive for many applications. The principle idea of this process is the use electrostatic force to fabricate fibers. Electrospinning solutions, at an appropriate concentration, which can perform polymer chain entanglement, are electrified by applying a positive potential against a grounded collector to create an electrostatic field. The nanofibers are formed and deposited on the collector as a non-woven fiber mat.

Although numerous polymeric nanofibers have been fabricated, poly(acrylic acid) (PAA) nanofibers by electrospinning have not been prepared to the same degree as other polymers [11,12]. PAA is a synthetic high molecular weight polymer of acrylic acid, which behaves like an anionic polymer according to its carboxylate group [13]. To fabricate PAA nanofibers, the operating parameters, solution concentration and solvent, applied voltage, distance between needle and collector, and flow rate of the polymer solution have to be optimized [14,15]. In order to prepare water insoluble PAA nanofibers, the electrospun PAA nanofibers are then crosslinked by thermally-induced esterification [16]. As the water-stable PAA nanofibers have many prominent properties, it is expected that PAA nanofibers incorporated with antibacterial agents can have a synergistic effect and be even more beneficial as a wound dressing that delivers a therapeutic antibacterial effect to a specific site.

There are several methods used to incorporate therapeutic compounds into nanofiber mats. These methods include coating, sorption, embedding, and encapsulating [17,18]. Even loading the therapeutic agents within the nanofibers during electrospinning is possible and produces high loading efficiency, despite the fact that the process is rather complex and there is a need to optimize the proper condition for each type of therapeutic compound. Moreover, a burst release profile can be obtained from a normal electrospinning process. There is also another method for loading therapeutic agents after the electrospinning procedure. This is a very simple and practical method, in which the nanofiber mats are completely immersed in a therapeutic agent solution and the drug is adsorbed on the surface and also absorbed within the electrospun nanofiber mats by simple physical sorption. A similar burst release behavior can then be obtained by both simultaneous and post-operative loadings [19].

In this work, the main objective was to fabricate thermally cross-linked PAA nanofiber mats, which contained a model drug doxycycline hyclate (hydrochloride hemiethanol hemihydrate of doxycycline; DOXY-h); a broad-spectrum antibiotic. Subsequently, the DOXY-h loaded-PAA (PAA/DOXY-h) nanofiber mats were characterized for morphology, actual drug content, adsorption isotherms, in addition to in vitro drug release behavior and release kinetics.

Antibacterial properties of the PAA/DOXY-h nanofiber mats against aerobic bacteria were investigated.

4.3 Materials and Methods

4.3.1 Materials

Poly(acrylic acid) (PAA; average $M_w = 450,000$ g/mol); doxycycline hyclate (DOXY-h; ≥ 98 % (TLC)); and ethylene glycol (anhydrous) were purchased from Sigma-Aldrich (USA). Ethyl alcohol was purchased from Decon (USA). Hydrosulfuric acid (H_2SO_4) was also purchased from Sigma-Aldrich (USA). Potassium chloride, sodium chloride, potassium phosphate monobasic, and sodium phosphate dibasic heptahydrate were supplied from Fisher Scientific (USA). All chemicals were used as received without further purification.

4.3.2 Preparation of Electrospinning Solution

Briefly, an electrospinning solution was prepared by dissolving PAA in ethanol to prepare a 4 wt% PAA solution under mechanical stirring until achieving a homogeneous solution. Next, ethylene glycol, a crosslink agent, was added to the PAA solution to obtain a concentration of 16 wt% and stirred continuously at ambient temperature for 24 h to complete dissolution. Immediately before the electrospinning process, 1M H_2SO_4 was added to the electrospinning solution at a concentration of 50 $\mu\text{g/mL}$ in order to catalyze the thermal crosslinking of the PAA nanofiber mats.

4.3.3 Fabrication of PAA Nanofiber Mats by Electrospinning Technique

PAA nanofiber mats were produced by the electrospinning method. The instruments used in the process consisted of a high voltage power supply (0-30 kV Spellman CZE1000R, Spellman High Voltage Electronics Corporation), a syringe pump (KD Scientific), and an adjustable-speed rotating stainless steel collector. The electrospinning solution was filled into a 5 mL syringe fitted with a stainless steel blunt needle (18-gauge), which was connected to the positive electrode. The grounding electrode was connected to a rotating stainless steel drum, or collecting device. The processing parameters such as electrical potential and needle tip-to-collector distance were fixed as 15 kV and 20-22 cm, respectively. The

volumetric flow rate of the electrospinning solution was set at 0.8 mL/h. All experiments were manipulated at 25 °C with humidity below 20 %. To obtain the water-insoluble PAA nanofiber mats, crosslinking was achieved through thermally-induced esterification at 130 °C within a vacuum for 30 min and cooled down to room temperature, then keep in an airtight package prior to further investigation.

4.3.4 Preparation of PAA/DOXY-h Nanofiber Mats

To load DOXY-h into the crosslinked PAA nanofiber mats, drug sorption, which is straightforward and practical, was selected in order to avoid any degradation of DOXY-h during the electrospinning process and thermo-crosslinking of the PAA nanofibers mats. Four models of PAA/DOXY-h nanofiber mats: PAA/DOXY-h125, PAA/DOXY-h250, PAA/DOXY-h500, and PAA/DOXY-h1000 were prepared by soaking crosslinked PAA nanofiber mats in a DOXY-h aqueous solution at a concentration of 125, 250, 500, or 1000 µg/mL, respectively. Airtight containers were used and wrapped with aluminum foil, then stored in a fridge overnight in order to achieve equilibrium drug absorption without any light or heat degradation. Finally, the PAA/DOXY-h nanofiber mats were withdrawn and excess DOXY-h solution was removed with tissue paper before further investigation.

4.3.5 Characterization and Testing

4.3.5.1 *Morphology Observations*

The morphology of the PAA nanofiber mats was examined using a scanning electron microscope (SEM; JSM-6510LV, JEOL). Before SEM operation, the specimens were sputter-coated with a thin layer (1 nm) of gold. Next, the samples were imaged using a secondary electron-image (SEI) detector at a magnification of 5000 with an operating voltage of 20 kV. The diameter of the nanofibers was also investigated directly from SEM images using Semafore 5.21 software. The thickness of the PAA nanofiber mats was measured by a micrometer (Fowler 52-545-001). At least 10 measurements on different areas of the nanofiber mats were observed to attain a data point ($n = 10$).

4.3.5.2 *Fourier Transform Infrared Spectroscopy*

The chemical compositions of PAA and PAA/DOXY-h nanofiber mats were analyzed by fourier transform infrared (FTIR) spectrometry (Nexus 670, Thermo Nicolet, USA) and recorded in the transmittance mode. The

PAA and PAA/DOXY-h nanofiber mats were placed on a horizontal attenuated total reflectance (HATR) plate with ZnSe under the following conditions: transmittance mode covering a broad range from 4000 cm^{-1} to 400 cm^{-1} at 64 scans with a resolution of 2 cm^{-1} at room temperature.

4.3.5.3 Determination of Drug Content, Adsorption Isotherm Data and In Vitro Drug Release Behavior

4.3.5.3.1 Preparation of Phosphate Buffer Saline Solution

Phosphate buffer saline (PBS) solution, at a pH condition of 7.4, was used as a releasing medium. To prepare a 20x concentration of PBS stock solution, 0.2 g of potassium chloride, 8 g of sodium chloride, 0.2 g of potassium phosphate monobasic, and 2.16 g of sodium phosphate dibasic heptahydrate were dissolved in distilled water. The volume was then adjusted to 50 ml with distilled water. Prior to further use, the 20x PBS solution needed to be diluted with distilled water to restore the typical working concentration (i.e., 1x PBS solution). The pH of the reconstituted buffer solution was 7.4.

4.3.5.3.2 Stability of DOXY-h in PAA/DOXY-h Nanofiber

The stability of DOXY-h in both the DOXY-h solution and within the PAA/DOXY-h nanofiber mats was observed by UV-VIS spectra of DOXY-h in the DOXY-h solution and the DOXY-h released from PAA/DOXY-h nanofiber mats (experimental conditions: sample dose = 2 mg/15 mL, contact time = 24 h, and temperature = 37 °C).

4.3.5.3.3 Adsorption Isotherms

Adsorption isotherms of DOXY-h on the PAA nanofiber mats were investigated to describe the interaction between the DOXY-h (adsorbate) and PAA nanofiber mats (adsorbent) at the equilibrium state. Langmuir and Freundlich mathematical models are normally used to predict the adsorption isotherms; therefore these two models were applied to analyze this system. The experiment included the preparation of the DOXY-h solution at various initial concentrations (40-1000 mg/L). Approximately 0.002 g of PAA nanofiber mat was added to each bottle containing 3 mL of DOXY-h solution at various concentrations. The bottles were shaken at 100 rpm, at temperature $\sim 8\text{ }^{\circ}\text{C}$ for 24 h to reach

equilibrium. The amount of DOXY-h in the solution before and after adsorption was assayed using a UV-VIS spectrophotometer at 351 nm.

4.3.5.3.4. Drug Content

The actual amounts of DOXY-h within the PAA/DOXY-h125, PAA/DOXY-h250, PAA/DOXY-h500, and PAA/DOXY-h1000 were quantified before the release assay. Briefly, the PAA/DOXY-h nanofiber mats were cut into small pieces and immersed in 3 mL distilled water then sonicated for 2 h to complete the extraction of DOXY-h from the PAA/DOXY-h nanofiber mats. The extraction solutions were evaluated for the amounts of DOXY-h by a UV-VIS spectrophotometer (Lambda 800, Perkin Elmer) at a maximum absorption wavelength of 351 nm. The experiments were assessed in triplicate and the results were presented as mean values.

4.3.5.3.5 DOXY-h Release Assay

The release study was performed by the total immersion method at 37 °C in PBS, as a medium. The PAA/DOXY-h nanofiber mats were cut into small pieces and immersed in 15 mL PBS in a tightly sealed vial with aluminum foil wrap to protect the specimens from light. The experiment was performed at 37 °C with agitation at 100 rpm using a compact incubator with orbital shaking (MaxQ Mini 4450, Thermo Scientific). At each immersion interval, ranging from 0 to 24 h, 3 mL of the aliquot releasing medium was sampled, and an equivalent amount of fresh PBS solution was added to provide a constant volume. The amount DOXY-h released was evaluated by a UV-VIS spectrophotometer at a specific wavelength of 351 nm. Three parallel studies were conducted and the results were presented as mean values. The obtained data were calculated using a predetermined calibration curve of DOXY-h (concentration range of 1.5625-100 µg/mL) to get the cumulative amount of the released DOXY-h from the PAA/DOXY-h nanofiber mats.

4.3.5.4 Anti-bacterial Determination

The antibacterial activity of the PAA/DOXY-h nanofiber mats was analyzed based upon the disc diffusion method of the US Clinical and Laboratory Standards Institute (CLSI), against aerobic bacteria generally found on the surface of human body, i.e., *P. aeruginosa* (gram-negative), *S. aureus* (gram-

positive) and *Streptococcus agalactiae* (gram-positive). The bacterial suspension, at a density equivalent to 0.5 McFarland (1.5×10^8 CFU/mL) was spread over the brain heart infusion (BHI) agar, trypticase soy agar, and blood agar plates for *P. aeruginosa*, *S. aureus* and *S. agalactiae*, respectively. The specimens were cut into 3 mm discs. PAA nanofiber mats without DOXY-h were used as a control. Each specimen was placed on microorganism-cultured agar plates and incubated at 37 °C for 24 h. The diameter of an inhibition zone in the agar plate was observed and measured after 24 h of incubation. The experiments were completed in triplicate to get the mean values.

4.4 Results and Discussion

4.4.1 Fabrication of PAA and PAA/DOXY-h Nanofiber Mats

The PAA nanofiber mats were easily fabricated by electrospinning of the 4 wt% PAA solution with ethylene glycol in ethanol under an applied voltage of 15 kV with the volumetric flow rate of the electrospinning solution at 0.8 mL/h over a collection distance of 20-22 cm. The appearance of the obtained electrospun mats was white opaque with an average thickness of ~40 μm (for the mats that were electrospun from 10 ml of the electrospinning solution). Figure 4.1 shows that the PAA nanofiber mat exhibits a multilayer, uniform structure with a smooth surface of nanofibers, without any bead, with a diameter of $\sim 330 \pm 66$ nm. Micro-size porous channels that are created from the random deposition of the fiber segments provide high porosity. These channels act paths for drug diffusion [20].

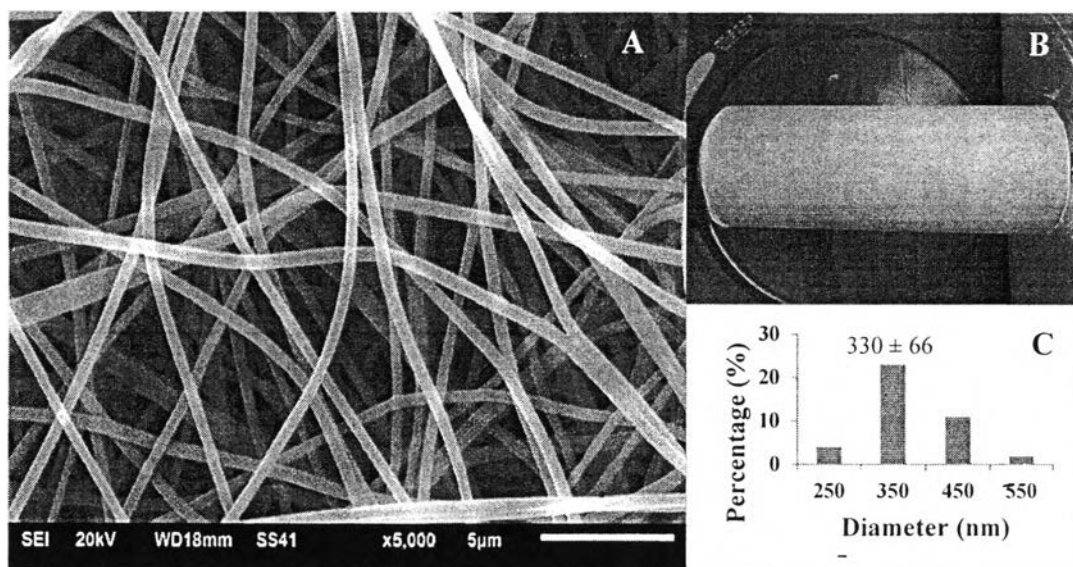


Figure 4.1 PAA nanofiber mats from 4 wt% PAA in ethanol solution containing 16% ethylene glycol at 15 kV after thermo-crosslinking: a) scanning electron micrograph at 5000x, b) photograph, and c) size distribution range and mean diameter of nanofibers.

4.4.2 FT-IR Analysis of DOXY-h, PAA, and PAA/DOXY-h Nanofiber

FT-IR analysis was performed on the DOXY-h, PAA, and PAA/DOXY-h nanofiber mats to identify characteristic absorption peaks corresponding to the chemical structures. For DOXY-h, absorption peaks around 3451 cm^{-1} , 3284 cm^{-1} , 1666 cm^{-1} are assigned to the hydrogen-bonded O-H stretch, N-H stretch, and C=O stretch vibration of the phenols, amides, and carbonyl group, respectively. For PAA, the ester bond absorption peaks, at 1705 cm^{-1} and 1253 cm^{-1} represented C=O and C-O, which verified the crosslinking via esterification of PAA. As hypothesized for the PAA/DOXY-h nanofiber mats, the main characteristic bands of both DOXY-h and PAA were present in the spectra without any new absorption peaks. It could be implied that there was no interaction between PAA and DOXY-h.

4.4.3 Sorption Isotherms, DOXY-h Content, and Release Profiles

The calibration curve of DOXY-h was prepared to determine the content of DOXY-h in the PBS. The obtained linear equation was:

$$y = 0.0239x - 0.0064 \quad (1)$$

where x is the concentration of DOXY-h and y is the absorbance (a correlation coefficient of 0.9999). The absorbance of DOXY-h was studied by UV-VIS spectrophotometry at 351 nm within the concentration of DOXY-h between 1.56–100 $\mu\text{g/ml}$.

The stability of DOXY-h in both the DOXY-h solution and within the PAA/DOXY-h nanofiber mats was observed spectrophotometrically to confirm whether drug degradation was occurred during the experiment. As shown in Figure 4.2, DOXY-h in the DOXY-h solution and the as-released DOXY-h solution shows similar UV-VIS spectra with insignificant differences in the absorbance. It could be suggested that DOXY-h was stable during the course of the experiment.

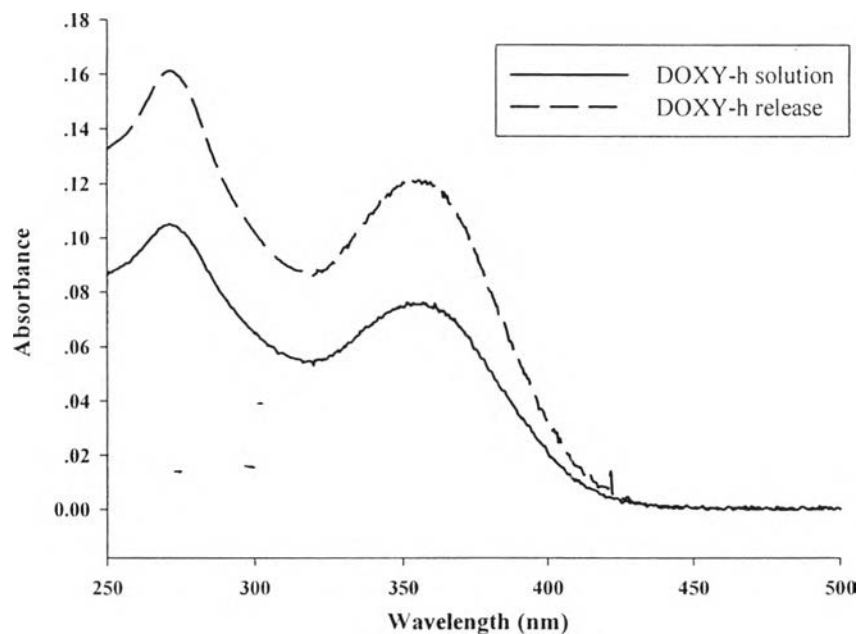


Figure 4.2 UV-VIS spectra of the DOXY-h in drug solution and DOXY-h released from nanofiber mats after 24 h of incubation at 37 °C. Experimental conditions: sample dose = 2 mg/15 mL, contact time = 24 h, and temperature = 37 °C).

The adsorption capacity of PAA nanofiber mats toward DOXY-h was investigated and the result is shown in Figure 4.3. The equilibrium adsorption capacities of the DOXY-h (q_e) increased upon increasing of the equilibrium concentration of the DOXY-h in the solutions (C_e). The adsorption isotherm was further analyzed using the linear form of Langmuir (Eq. 2) and the Freundlich models (Eq. 3):

$$\frac{1}{q_e} = \frac{1}{q_m K_L C_e} + \frac{1}{q_m} \quad (2)$$

$$\log q_e = \frac{1}{n} \log C_e + \log K_F \quad (3)$$

where q_e is the amount of DOXY-h adsorbed per unit weight of PAA nanofiber mats at equilibrium (mg/g), q_m is the maximum adsorption capacity for forming a single layer (mg/g), C_e is the equilibrium concentration of DOXY-h remaining in the solution when the amount adsorbed was equal q_e (mg/L), K_L is the Langmuir constant (L/mg), and is related to the energy or net enthalpy of adsorption, and K_F is the Freundlich constant ((mg/g)(L/mg)^{1/n}), which is related to the adsorption capacity. Figure 4.3 also demonstrates the Langmuir and Freundlich models fitting. The adsorption isotherm parameters determined from the slopes and intercepts of the plots are shown in Table 4.1. The appropriate model of the adsorption isotherm parameters can be estimated by the correlation coefficient (R^2), which is close to 1. Hence, the Freundlich adsorption isotherm was more favorable to the adsorption of DOXY-h, with the highest value of $R^2 = 0.9888$. This result reveals that the adsorption of DOXY-h on the PAA nanofiber mat surface is a physical adsorption according to value of $n > 1$.

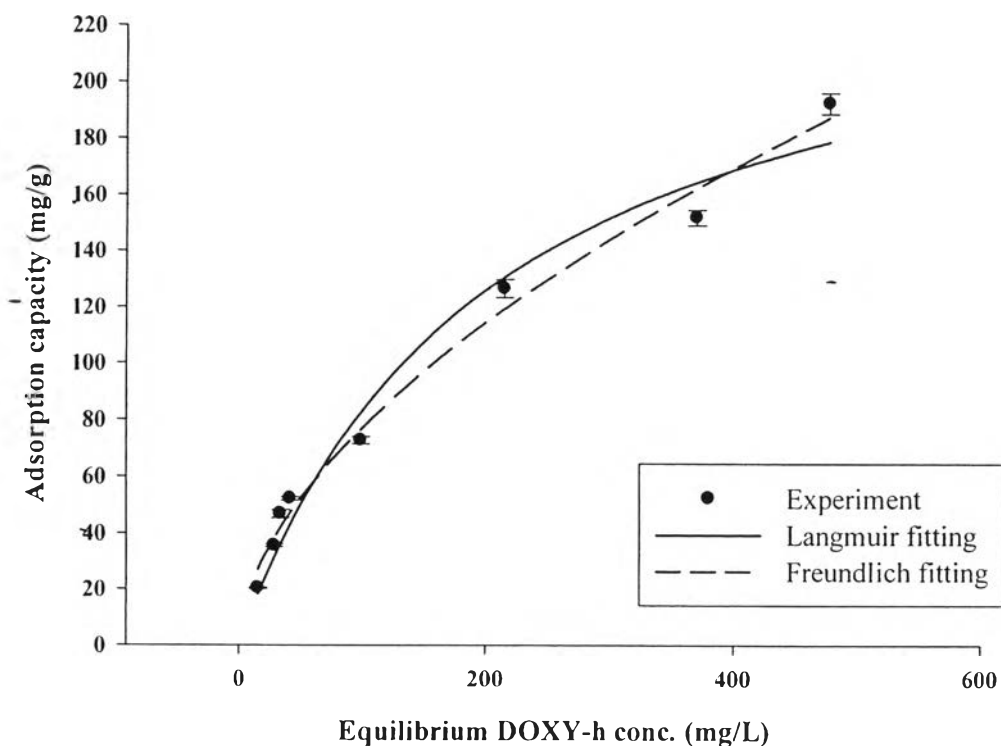


Figure 4.3 Adsorption isotherm of DOXY-h onto PAA nanofiber mats.

Table 4.1 Amount of model drugs within PAA/DOXY-h nanofiber mats

Langmuir isotherm			Freundlich isotherm		
q_m (mg/g)	K_L (L/mg)	R^2	K_F (mg/g)(L/mg) ^{1/n}	n	R^2
256.4117	0.0048	0.9750	5.6895	1.7652	0.9888

The actual amounts of DOXY-h are important parameters to determine the properties of the drug-loaded nanofiber mats. Table 4.2 shows the actual amount of the DOXY-h present in the specimens. The actual amount of DOXY-h present in PAA/DOXY-h125, PAA/DOXY-h250, PAA/DOXY-h500 and PAA/DOXY-h1000 ranged between 27.57 mg/g to 101.71 mg/g of PAA nanofiber

mats. It is apparent that the drug content in PAA nanofiber mats significantly increased with increasing drug loading in the soaking solution.

Table 4.2 Adsorption isotherm parameters for the adsorption of PAA/DOXY-h nanofiber mats

Nanofiber mat	Actual amount of DOXY-h per weight of fiber (mg/g)
PAA/DOXY-h125	27.57
PAA/DOXY-h250	45.38
PAA/DOXY-h500	66.27
PAA/DOXY-h1000	101.71

The *in vitro* drug release profile of the DOXY-h for the four PAA/DOXY-h nanofiber mats is illustrated in Figure 4.4. It is evident that all four PAA/DOXY-h nanofiber mat models exhibit an initial burst release characteristic of a cumulative ranging between 37.14 % and 45.97 %. Corresponding to the actual amount of drug within PAA nanofiber mats, the cumulative percentage of the DOXY-h increased while increasing the actual amount of drug in the PAA/DOXY-h nanofiber mats. The initial burst release could possibly be due to the extreme release of the physically adsorbed drug present on the surface of the fiber mats when exposed to the releasing medium and the highly porous PAA nanofiber mats that allowed the diffusion of drug entrapped in the nanofibers. In the later phase of release, the drug diffused at a reduced rate due to the lower concentration of DOXY-h remaining in PAA nanofiber mats, and the elevated DOXY-h concentration in the release medium. Interestingly, that burst release of drug is accepted as an ideal drug release profile in the anticipation of postoperative infections, which usually happens within the first few hours after surgery [21].

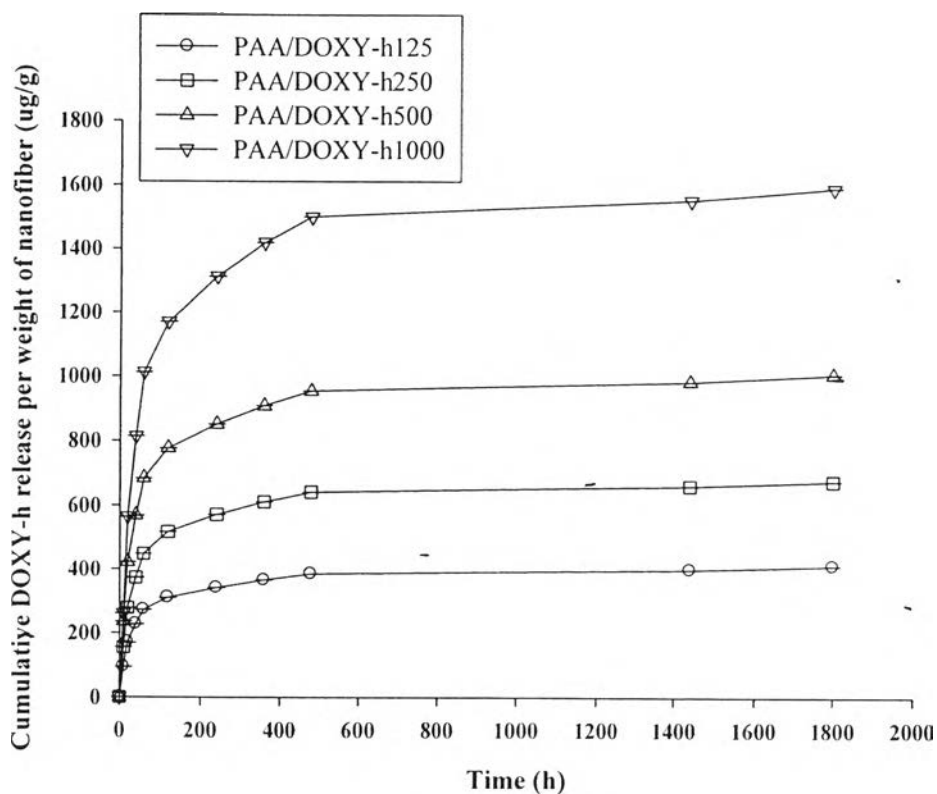


Figure 4.4 Cumulative release profiles of DOXY-h from PAA/DOXY-h nanofiber mats. The error bars represent the standard deviation based on triplicate analysis (* $p < 0.05$).

In addition, to verify the release kinetics of DOXY-h from the PAA/DOXY-h nanofiber mats, data obtained from the in vitro drug release study were applied using the following kinetic models:

$$\text{Zero-order model} \quad Q_t = Q_0 + K_0 t \quad (4)$$

where Q_t is the amount of drug dissolved in time, t , Q_0 is the initial amount of drug in the solution ($Q_0 = 0$), K_0 is the zero order release constant expressed in units of concentration/time and t is the release time,

$$\text{First order model} \quad \log C = \log C_0 - (Kt/2.303) \quad (5)$$

where C_0 is the initial concentration of drug and K is the first order rate constant, and

$$\text{Higuchi model} \quad Q = K_H \times t^{1/2} \quad (6)$$

where Q is the amount of drug released in time t , K_H is the Higuchi dissolution constant.

$$\text{Korsmeyer-Peppas model} \quad M_t/M_\infty = K t^n \quad (7)$$

where M_t / M_∞ is a fraction of drug released at time t , K is the release rate constant and n is the release exponent. The n value = 0.5 or less indicates Fickian diffusion, while $0.5 < n < 1$ indicates a non-Fickian model (anomalous mass transfer).

The release kinetic analysis based on the Higuchi model gave the highest correlation coefficients, which indicates that all the four models of PAA/DOXY-h nanofiber mats exhibited Fickian diffusion mechanism. It can be concluded that the DOXY-h release was governed by diffusion of the drug from the nanofibers [22]. Concurrently, the release exponent in Eq. 7 is ~ 0.5 . The release of DOXY-h from the PAA/DOXY-h nanofiber mats is primarily by drug desorption from the nanofiber surface [23].

4.4.4 Antibacterial Activity Evaluation

Antibacterial activity of the PAA/DOXY-h nanofiber mats were qualitatively evaluated against aerobic bacteria, i.e., *P. aeruginosa* (gram-negative), *S. aureus* (gram-positive) and *S. agalactiae* (gram-positive) according to the disc diffusion method. The 3-mm disc specimens of the PAA/DOXY-h nanofiber mats were placed on an agar plate seeded with cultures (300 μ l) and incubated for 24 h. The discs without DOXY-h served as controls. No inhibition zone was observed around the control disc on any tested bacterial strains. Results of disc diffusion assay are presented in Figure 4.5. According to the sizes of the inhibition zones, gram-positive bacteria; *S. aureus* and *S. agalactiae*, appeared to be more sensitive to PAA/DOXY-h nanofiber mats than gram-negative bacteria; *P. aeruginosa*, as shown in Figure 4.6. Among the tested organisms, *S. aureus* showed sensitivity levels

toward PAA/DOXY-h nanofiber mats almost similar to that of *S. agalactiae*. In addition, the antimicrobial activities of the PAA/DOXY-h nanofiber mats against gram-positive bacteria are slightly independent of the drug concentration between DOXY-h 125, 250, 500 and 1000 $\mu\text{g/ml}$. However, the inhibition zone of the PAA/DOXY-h nanofiber mats against gram-negative bacteria; *P. aeruginosa* was drug concentration dependent.

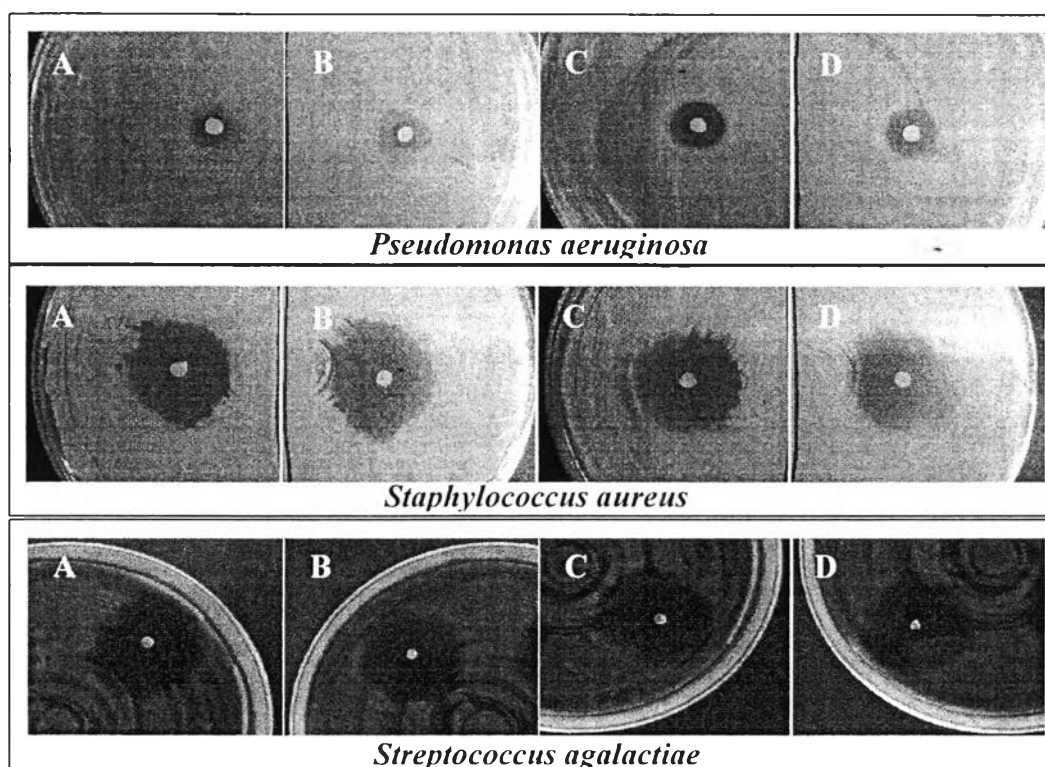


Figure 4.5 Disc diffusion assay of the electrospun PAA/DOXY-h nanofiber mats: a) PAA/DOXY-h125, b) PAA/DOXY-h250, c) PAA/DOXY-h500, and d) PAA/DOXY-h1000 against gram-negative bacteria; *P. aeruginosa* and gram-positive bacteria; *S. aureus* and *S. agalactiae*.

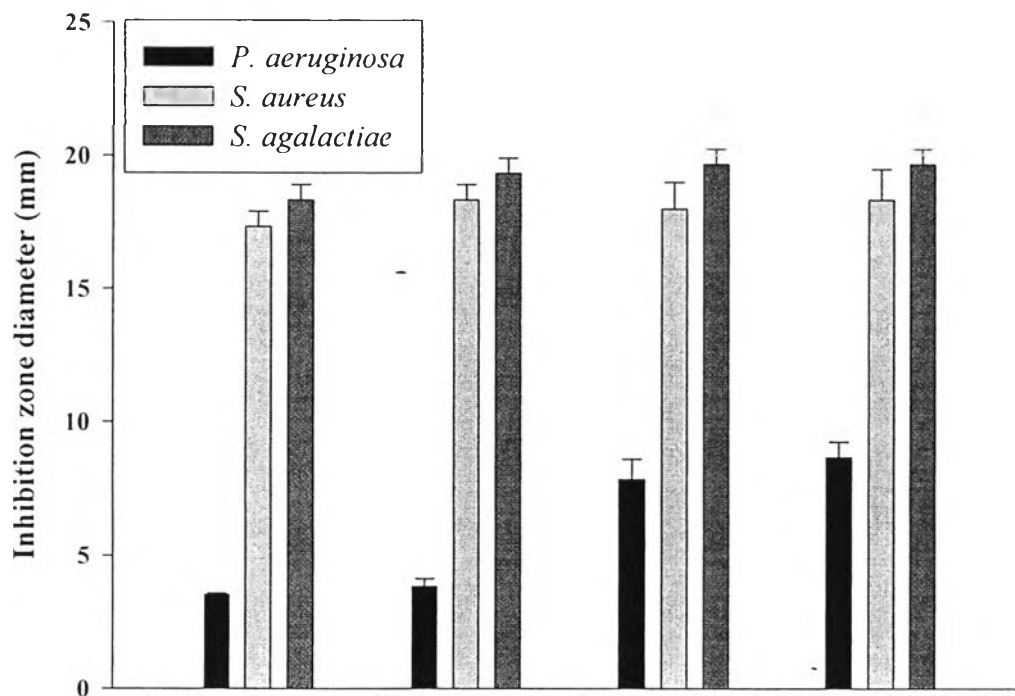


Figure 4.6 Inhibition zone of DOXY-h loaded-PAA nanofiber mats against three strains of bacteria.

4.5 Conclusions

PAA/DOXY-h nanofiber mats were fabricated using the electrospinning technique, then the drug at various doses of DOXY-h, was loaded by a simple drug absorption method. It was observed that the DOXY-h content in the PAA nanofiber mats significantly increased when DOXY-h in soaking solution increased. The adsorption isotherms for the adsorption of DOXY-h were representative of the Freundlich model. The release properties of DOXY-h from the PAA/DOXY-h nanofiber mats under physiological conditions exhibited an initial burst release characteristic, which was governed by the Fickian diffusion mechanism. These particular nanofiber mats demonstrated antibacterial properties against gram-positive bacteria; *S. aureus* and *S. agalactiae*, and appeared to be more effective than against gram-negative bacteria; *P. aeruginosa*. The PAA/DOXY-h nanofiber mats, due to

their simple fabrication process, release characteristics and antibacterial properties, could be used for wound dressing applications.

4.6 Acknowledgements

The author would like to thank and give appreciation to my advisor, Professor Pitt Supaphol, for his valuable recommendations, helpful discussions, encouragement, and kindness throughout my graduate study at the Petroleum and Petrochemical College, Chulalongkorn University, Thailand. The author wishes to acknowledge the Petroleum and Petrochemical College (Chulalongkorn University), Department of Macromolecular Science and Engineering (Case Western Reserve University), and Department of Ophthalmology & Visual Science Research Center (Case Western Reserve University) for making this research possible.

4.7 References

1. Cogen AL, Nizet V, Gallo RL (2008) Skin microbiota: A source of disease or defence? *British Journal of Dermatology* 158 (3):442-455
2. Normal Microbial Flora of the Human Body.196-201
3. Understanding Emerging and Re-emerging Infectious Diseases (2007). National Institutes of Health
4. White R, Cutting KF (2006) Modern exudate management: A review of wound treatments. *World Wide Wounds* 1
5. Kanani AG, Bahrami SH (2010) Review on electrospun nanofibers scaffold and biomedical applications. *Trends Biomater Artif Organs* 24 (2):93-115
6. Huang ZM, Zhang YZ, Kotaki M, Ramakrishna S (2003) A review on polymer nanofibers by electrospinning and their applications in nanocomposites. *Composites Science and Technology* 63 (15):2223-2253
7. Huang L, Nagapudi K, P. Apkarian R, Chaikof EL (2001) Engineered collagen-PEO nanofibers and fabrics. *Journal of Biomaterials Science, Polymer edition* 12 (9):979-993

8. Li WJ, Laurencin CT, Caterson EJ, Tuan RS, Ko FK (2002) Electrospun nanofibrous structure: A novel scaffold for tissue engineering. *Journal of Biomedical Materials Research* 60 (4):613-621
9. Matthews JA, Wnek GE, Simpson DG, Bowlin GL (2002) Electrospinning of collagen nanofibers. *Biomacromolecules* 3 (2):232-238
10. Park H-S, Park YO (2005) Filtration properties of electrospun ultrafine fiber webs. *Korean Journal of Chemical Engineering* 22 (1):165-172
11. Kim B, Park H, Lee S-H, Sigmund WM (2005) Poly(acrylic acid) nanofibers by electrospinning. *Materials Letters* 59 (7):829-832
12. Li L, Hsieh Y-L (2005) Ultra-fine polyelectrolyte fibers from electrospinning of poly(acrylic acid). *Polymer* 46 (14):5133-5139
13. Atchison JS, Schauer CL (2012) Fabrication and Characterization of Electrospun Pristine and Fluorescent Composite Poly (acrylic acid) Ultra-Fine Fibers. *Journal of Engineered Fabrics & Fibers (JEFF)* 7 (3)
14. Thompson CJ, Chase GG, Yarin AL, Reneker DH (2007) Effects of parameters on nanofiber diameter determined from electrospinning model. *Polymer* 48 (23):6913-6922
15. Theron SA, Zussman E, Yarin AL (2004) Experimental investigation of the governing parameters in the electrospinning of polymer solutions. *Polymer* 45 (6):2017-2030
16. Xiao SL, Shen MW, Ma H, Guo R, Zhu MF, Wang SY, Shi XY (2010) Fabrication of water-stable electrospun polyacrylic acid-based nanofibrous mats for removal of copper (II) ions in aqueous solution. *Journal of Applied Polymer Science* 116 (4):2409-2417
17. Taepaiboon P, Rungsardthong U, Supaphol P (2006) Drug-loaded electrospun mats of poly(vinyl alcohol) fibres and their release characteristics of four model drugs. *Nanotechnology* 17 (9):2317-2329
18. Suwantong O, Ruktanonchai U, Supaphol P (2010) In vitro biological evaluation of electrospun cellulose acetate fiber mats containing asiaticoside or curcumin. *Journal of Biomedical Material Research Part A* 94 (4):1216-1225

19. Zong X, Kim K, Fang D, Ran S, Hsiao BS, Chu B (2002) Structure and process relationship of electrospun bioabsorbable nanofiber membranes. *Polymer* 43 (16):4403-4412
20. Park CG, Kim E, Park M, Park JH, Choy YB (2011) A nanofibrous sheet-based system for linear delivery of nifedipine. *Journal of the Controlled Release* 149 (3):250-257
21. Fang J, Wang X, Lin T (2011) Functional applications of electrospun nanofibers. *Nanofibers-Production, Properties and Functional Applications*:287-326
22. Sill TJ, von Recum HA (2008) Electrospinning: Applications in drug delivery and tissue engineering. *Biomaterials* 29 (13):1989-2006
23. Pillay V, Dott C, Choonara YE, Tyagi C, Tomar L, Kumar P, du Toit LC, Ndesendö VMK (2013) A review of the effect of processing variables on the fabrication of electrospun nanofibers for drug delivery applications. *Journal of Nanomaterials* 2013:1-22